Multi-View Continuous Structured Light Scanning

Fabian Groh, Benjamin Resch, Hendrik P. A. Lensch

University of Tübingen

Abstract. We introduce a highly accurate and precise multi-view, multi-projector, and multi-pattern phase scanning method for shape acquisition that is able to handle occlusions and optically challenging materials. The 3D reconstruction is formulated as a two-step process which first estimates reliable measurement samples and then simultaneously optimizes over all cameras, projectors, and patterns. This holistic approach results in significant quality improvements. Furthermore, the acquisition time is drastically reduced by relying on just six high-frequency sinusoidal captures without the need of phase unwrapping, which is implicitly provided by the multi-view geometry.

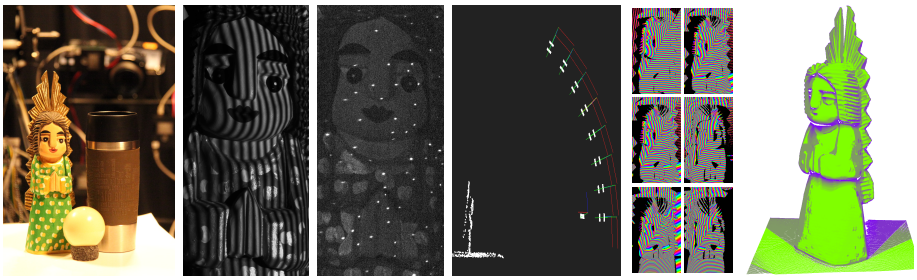

(a) (b) (c) (d) (e) (f)

Fig. 1: For objects (a) with optically challenging properties, shifted sinusoidal patterns (b) are captured from multiple cameras and projectors. On top of the phase information, highly accurate features (c) are generated to perform a precise bundle adjustment (d). With the multi-view continuous phase signals (e) the reliable camera-projector pairs for every surface point are estimated by validating multi-view consistency (f). Finally, we optimize the depth over all available information.

1 Introduction

In order to capture a complete model and to provide a good coverage of the visible surface area of any real-world object, a multi-view approach is neces-

sary. In particular, these multi-view recordings are relevant in the context of object recognition, industrial inspection and material acquisition where also the illumination is varied. In all applications, it is beneficial to acquire a detailed geometry model to establish precise correspondences between the different views. In this paper, we propose an active multi-view, multi-projector shape acquisition system.

Multi-view acquisition systems typically consist of multiple cameras that are either distributed at fixed positions [21], or are movable [1] around an object, or get extended with projectors to perform active structured light (SL) scanning alongside reflection measurements [24]. While our proposed method is developed to be used inside such an illumination system for material acquisition, it purely focuses on achieving high-quality active SL geometry reconstruction in the general case of multiple viewpoints. In this case, each projector-pattern produces a continuous SL signal that is captured by every camera as a two-dimensional projection. The main idea is that a surface point is located exactly where all SL signals from different viewpoints align, provided that the surface is visible from the respective camera-projector pair and the signal is not corrupted by material properties like specular- or inter-reflections.

To surpass the projector resolution, which is the most limiting factor of SL scanning, continuous coding methods [20] are suggested. We use traditional phase shifting methods (PS), where phases are recovered from projecting at least three shifted sinusoidal patterns [23]. Phase shifting methods have been proven to deliver high-quality results with sub-pixel accuracy, even in optically difficult areas [5, 6, 14, 17]. We fully integrate phase shifting into our multi-view reconstruction pipeline with two benefits. The multi-view approach further improves the accuracy, and we can eliminate the need for explicit phase unwrapping by a multi-view consistency validation. Thus, our method just needs to capture the highest frequency patterns. Real world objects are often composed out of different materials with varying illumination profiles, which make it necessary to capture the phase shifting patterns in high dynamic range (HDR) sequences to achieve precise results in all areas.

Since our optimization requires correct camera and projector poses, a very accurate calibration is required. We perform a precise online bundle adjustment (BA) on actively marked corresponding points. Therefore, we propose to combine the HDR phase shifting results with a fast LDR projector pixel identification scheme to get highly accurate sub-pixel correspondences for a structure from motion reconstruction.

The presented results feature a geometry accuracy far beyond the pixel resolution of both the involved cameras and projectors.

2 Related Work

3D Reconstruction: Three-dimensional shape estimation from real world objects is still a very challenging task and an active field of research. In general, methods can be classified into two major categories: namely passive and active. In

passive approaches, the scene is just captured from at least two viewpoints. The most prominent representatives are multi-view stereo systems. However, most of these techniques depend heavily on finding good salient point correspondences between the views. Thus, they have problems in optically challenging and textureless areas that often results in sparse reconstructions. A comparison and evaluation can be found in [22].

Active techniques overcome this issue by establishing correspondences between camera and projector pixels for each scene point with active illumination patterns. Besides laser scanning [4], projector-based structured light pattern are a well-studied technique [7,20]. The projected patterns establish correspondences on the object, in the way that every point has a corresponding code-word, which can be recovered by analyzing the differences in the captured images with the projected patterns. Salvi et al. [20] compare state of the art structured light patterns.

Structured light scanning in the appearance of global illumination, interreflections or challenging materials, e.g. specular reflections, can still be an issue. High frequency patterns can cope with that kind of problems [5,6,17]. Gupta et al. [14] propose to combine different Gray code patterns logically in an ensemble. This method achieves remarkable results. Nevertheless, the used patterns just provide a discrete coding, and in consequence are not able to surpass the projector resolution on their own. Hence, they applied the same technique to a phase shifting method as Micro PS [15].

In traditional approaches, structured light patterns need to be temporally unwrapped by projecting coarse-to-fine patterns consecutively to get a unique correspondence for each point. The disadvantage is the number of additional patterns that are dependent on the projector resolution. In the context of phase shifting methods, this is referred to as phase unwrapping [20], where each frequency band needs to be captured by at least three shifts. Multiple methods are addressing this issue by reducing the amount of necessary patterns [20], e.g. Embedded PS [16], and Micro PS [15]. Our approach replaces phase-unwrapping by exploiting the multi-view setup.

Multi View Structured Light Scanning: For the purpose of phase unwrapping in a stereo camera plus projector system, Garcia and Zakhor [11] present a method that performs a correspondence labeling in the projector domain via loopy belief propagation. Afterwards, missing absolute phases are estimated in the camera domain from neighboring pixels.

Binary structured light scanning from uncalibrated viewpoints has been proposed by several approaches: with a laser pointer [8], for multiple viewpoints [9, 13], and for multiple projectors in a one-shot setting [10]. In a setting with multiple cameras Young et al. [25] suggest using viewpoint-coded structured light to mimic the temporal encoding. In recent years, using multiple cameras and multiple projectors to capture geometry alongside photometric data in self-calibrating systems has been demonstrated by the work of Aliaga et al. [2,3] and Weinmann et al. [24]. Aliaga et al. utilize the projectors as additional virtual

cameras. While this is beneficial in settings with few cameras, it makes their approach even more dependent on the projector resolution. For a denser surface, they perform an up-sampling scheme by warping the photometric captures onto the geometrical model [2, 3]. Weinmann et al. [24] suggest utilizing overlapping areas of the projected binary codes from multiple projectors to overcome low projector resolutions. The final resolution of the surface area is directly dependent on the overlapping alignment of the projector pixel on the scene.

In contrast, our method utilizes traditional single phase shifting to achieve continuous signals in the scene [23]. Thus, it is possible to optimize directly on the continuous signals from multiple camera-projector pairs to estimate the surface. Further, we introduce a novel multi-view consistency validation that substitutes phase unwrapping, relies solely on high-frequencies patterns at no additional cost, and reliably handles occlusions. All calculations can be done for each 3D point separately without neighboring information. Additionally, we propose to enhance active sparse bundle adjustment with the continuous signal for better multi-view precision.

3 Multi-View Depth Optimization

Our reconstruction pipeline makes use of phase shifting patterns for two steps: Once, to establish active correspondence to perform a highly accurate bundle adjustment to estimate the camera and projector locations, and, second, for optimizing the 3D geometry.

For the actual depth estimation, at first, a viewpoint consistency validation is completed by coarsely sampling potential depth values. This step performs an explicit multi-view phase unwrapping by utilizing geometrical constraints. The step identifies for each pixel which camera-projector pairs provide valid samples. Subsequently, all points are further optimized solely on the reliable phase signal to achieve highly precise and accurate depth information. Figure 1 shows examples of the specific steps.

3.1 Multi-View HDR Continuous SL Calibration

This section describes our combination of the HDR phase scanning with an active sparse bundle adjustment (SBA). Initially, we calculate the phase responses for a horizontal and vertical projector pattern direction. Afterwards, sub-pixel accurate feature points are generated by utilizing phase responses. These precisely positioned feature points establish exact correspondences between all cameras and all projectors suitable for a high-precision SBA.

We perform this calibration online during the capturing process to estimate all extrinsic and also intrinsic parameters for a moving camera setup. In a fixed system the same calibration could also be performed as a pre-processing step.

HDR Phase Scanning: We use traditional phase shifting [5, 20] for the x and y directions of the projectors respectively. Given a linearized projector, a set of

N shifted sine patterns $L_{n,x}$ in direction x, period T is generated:

$$L_{n,x}(x,y) = 0.5\,\cos\left(x\,\omega + \theta_n\right) + 0.5, \tag{1}$$

with $\omega = {}^{1}/_{T}$ and $\theta_n = {}^{n2\pi}/_{N}$.

Once successively projected and captured by the camera the phase vector $\boldsymbol{u} = [o, c, s]$ (offset, cosine, sine) can be recovered for a single frequency given the captured intensity responses $\boldsymbol{r} = [r_0, r_1, \ldots, r_n]$ (see [16]):

$$\boldsymbol{u} = \underset{u}{\operatorname{argmin}} \|\boldsymbol{r} - A\boldsymbol{u}\|_2\,, \quad \text{with } A \coloneqq \begin{bmatrix} 1 & \cos(\theta_0) & -\sin(\theta_0) \\ 1 & \cos(\theta_1) & -\sin(\theta_1) \\ \vdots & \vdots & \vdots \\ 1 & \cos(\theta_n) & -\sin(\theta_n) \end{bmatrix}. \tag{2}$$

The phase ϕ is obtained by $\phi = \tan^{-1}\left({}^{s}/_{c}\right)$.

Since our goal is to recover the shape of objects with optically challenging materials, the acquisition with a HDR sequence is essential, for which we use the algorithm provided by Granados et al. [12].

Representing Phase Information: All phase differences and interpolations in this work are computed on the respective sine and cosine part, not on the angle. Consequently, for two phase responses a and b, we represent the norm as:

$$\|a - b\|_{\Phi} \coloneqq \sqrt{\left(\cos\left(a\right) - \cos\left(b\right)\right)^2 + \left(\sin\left(a\right) - \sin\left(b\right)\right)^2}\,, \tag{3}$$

and for linear interpolation:

$$lerp(a, b; \lambda)_{\Phi} \coloneqq \begin{bmatrix} (1-\lambda) * \cos(a) + \lambda \cdot \cos(b) \\ (1-\lambda) * \sin(a) + \lambda \cdot \sin(b) \end{bmatrix}. \tag{4}$$

While this approximation introduces errors on larger intervals, on small scale they perform close to the optimum. This is sufficient, since higher differences are thresholded and interpolation is most likely performed on very small scale. Especially on GPUs, this not only avoids unnecessary branching when dealing with phase values, but also enables the utilization of the texture hardware.

Active Sparse Bundle Adjustment: After capturing the phases patterns for each viewpoint, a sparse set of randomly sampled projector pixels are projected temporally onto the scene using a binary encoding to enumerate these pixels. This is very robust and done in LDR with high gain to be much faster than a single capture of a HDR sequence.

For the selected projector pixels the analytic phase is known. An initial camera pixel position for these feature points is obtained as the center of mass of the detected spots. Afterwards the the sub-pixel location is refined by the Nelder-Mead procedure [18] to match the analytically given phase to the measured phase in the camera image. This optimization procedure yields very accurate correspondences and subsequently more precise results in the SBA. For the SBA we use the work from [19].

3.2 Multi-View Depth Optimization

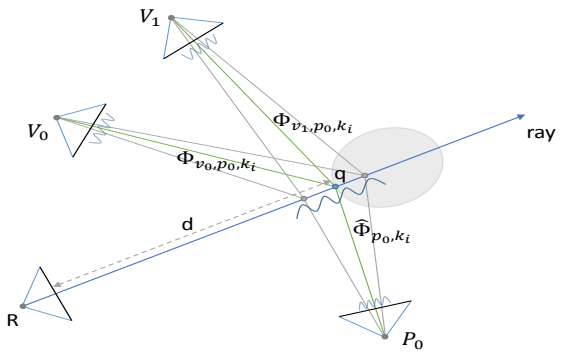

Fig. 2: General concept: Points along a ray are projected into all view-projector pairs. Each point is evaluated based on the phase differences between the obtained and the expected phase values for all patterns.

The general concept of our shape reconstruction is to recover the depth of a surface point by a multi-view optimization, i.e. combining the information of all cameras, projectors and patterns. Tracing a ray into the scene from an arbitrarily chosen reference camera system R, we are able to project any point q of depth d along the ray into all camera-views V and projectors P to get the respective phase responses $\Phi_{v,p,k}$ as well as the expected projector phases $\hat{\Phi}_{p,k}$ for all patterns K. This procedure is illustrated in Figure 2. For an actual surface point the phase differences $\|\Phi_{v,p,k}(d) - \hat{\Phi}_{p,k}(d)\|_{\Phi}$ are required to be minimal. However, we need to ensure to only operate on correct phase signals, since occlusion and optical properties could induce corrupted phase information. Hence, the depth reconstruction can be formulated as an optimization problem over all views, projectors and patterns:

$$d = \underset{d}{\operatorname{argmin}} \sum_{p \in P} \sum_{v \in V} \sum_{k \in K} \Omega_{v,p,k}(d) \, \|\Phi_{v,p,k}(d) - \hat{\Phi}_{p,k}(d)\|_{\Phi} \,, \tag{5}$$

where $\Omega_{v,p,k}(d)$ is our multi-view consistency validation that evaluates to 1 if the phase information is estimated to be reliable and 0 otherwise.

Multi-view Consistency Validation: This step identifies which phase responses are reliable. For that reason, correct phase responses need to be distinguished from false positives. These wrongly predicted phase signals occur very often in a system that only relies on high frequency patterns. On the other side, phase responses can also be truly wrong or corrupted by optical influences such as inter-reflections (false negatives). As neither of those signals should be used

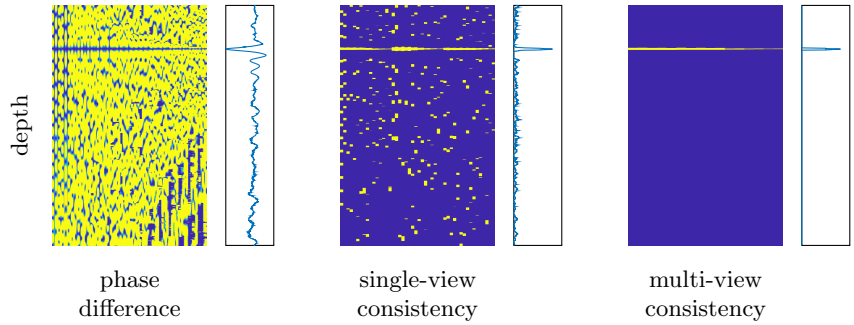

Fig. 3: Evaluation for an example point along a ray (depth) with the error/consistency for all camera-projector-pattern phase signals (horizontal) and the sum of each depth. Our multi-view consistency scheme is able to determine the contributing camera-projector pairs reliably and eliminates all false candidates.

for the optimization, it is necessary to keep track of such events to not falsely exclude cameras or projectors.

We utilize the geometrical setup to perform a consistency check. The acceptance measure of a single pattern is defined as:

$$\hat{\Omega}_{v,p,k}(d) \coloneqq \begin{cases} 1, & \text{if } \|\Phi_{v,p,k}(d) - \hat{\Phi}_{p,k}(d)\|_{\Phi} < \theta \\ 0, & \text{otherwise} \end{cases}, \tag{6}$$

where θ is the allowed threshold difference for a phase value to still be acceptable.

Further, for the correct depth all patterns from the same view-projector pair need to be consistent as well: $\hat{\Omega}_{v,p,k_0}(d) \wedge \cdots \wedge \hat{\Omega}_{v,p,k_{K-1}}(d)$ (single-view consistency).

Finally, we consider the fact that for any point in the scene it is not possible to have disjunctive subsets of valid view-projector pairs: If a projector is valid in one view it cannot be occluded in the other views; and vice versa. If a view is able to receive the signal from one projector this view cannot be occluded for the other projectors. Firstly, the contributing projectors are determined by evaluating the overlap of valid views. Subsequently, a view is accepted if it is valid for at least half of the contributing projectors. In that way, we allow for some optical disturbances. Nonetheless, corrupted phase responses are still excluded from the final optimization. The validation for a single point at different depth is demonstrated in Figure 3.

Coarse Approximation and Multi-view-based Phase Unwrapping: For the purpose of finding points close to a surface, the number of consistent phases correlates to a good alignment. Thus, performing multi-view consistency validation along the depth substitutes phase unwrapping.

With relaxing the consistency threshold θ, it is possible to coarsely sample the depth along the ray to approximate a good initial alignment.

Fine Depth Estimation: Our fine depth estimation takes the result of the coarse approximation as seed and performs a simple binary search on Equation 5. We compute the variance σ of the phase differences for the final depth as an additional measure of fitness.

4 Experimental Hardware Setup

All experiments in this paper have been captured in a light stage setting, with two Point Grey Grasshopper3 (GS3-U3-120S6C-C) 12 MP cameras and three Viewsonic Pro9000 1080p LED projectors. The two cameras are moved along an arc at about 1 m distance around the scene to different positions. They are treated as independent cameras in our system. The projectors have to be placed outside the light stage. Otherwise, they would occlude lightpaths for the reflectance measurement. Thus, their distance is roughly 1.40 m, and the scene is only covered by a subset of the projected area for each projector. The projector resolution on the scene is only about 500 µm, whereas the camera has a resolution of about 80 µm on the object. The setting is shown in Figure 5.

For the structured light scanning, we use two shifted sinusoidal patterns in horizontal as well as vertical direction respectively with a period length of 8 pixels and three shifts. Hence, we need to capture 6 HDR sequences per projector. We chose to capture the scenes from 8 positions along the two-camera-arc with an angle of about 10 degrees apart (vertical) and with the three projectors to the side (horizontal). Altogether, we optimize on 48 camera-projector pairs with two patterns each which result in 96 phases signals. For the demonstration of the results, we always choose the lowest camera viewpoint as the reference view. The global threshold for acceptable points is 8 camera-projector pairs and only phase differences below $\theta = \pi/6$ are considered acceptable. The coarse estimation is calculated in 100 µm steps.

Since all work is done on a per point basis, the problem is highly parallelizable. The optimization is carried out on the GPU requiring just a few seconds of computation time for a whole scene.

5 Results

In this section, we demonstrate our results on three objects that are shown in Figure 5. The angel is carved out of wood and painted in different colors. The small gold plates are a specular alloy. The mug consists of a plastic top and a rubber middle part with embossed details. In between and at the ground it consists of brushed metal. The ball is a good target since it features specular reflection as well as subsurface scattering; Furthermore, the diameter is known for ground truth evaluation.

Firstly, we demonstrate that our coarse depth estimation finds correct regions and respective visibilities. The colored point clouds are shown in Figure 4. Bright green areas display that all camera-projector pairs are reliable, whereas the darker regions indicate a drop of supported pairs. Keep in mind that the

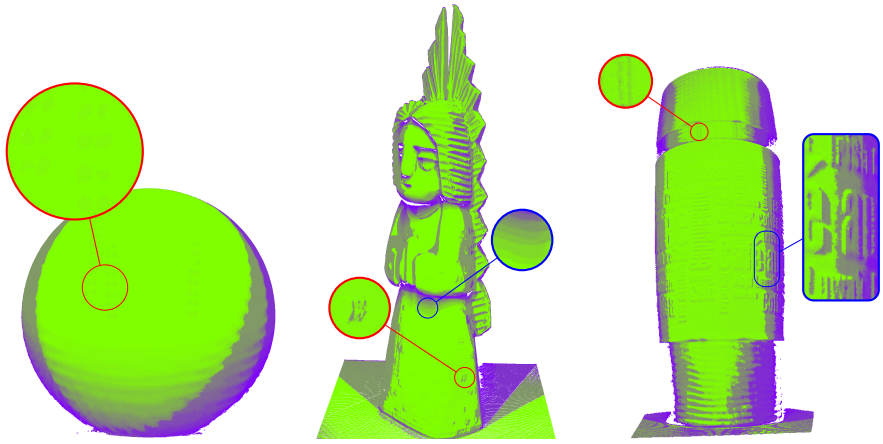

Fig. 4: Pointclouds of the estimated depth with respect to a reference camera. The color encodes the number of contributing camera-projector pairs: green (all) to purple (few). Changes are due to excluding unreliable phase information. Examples are given for specular reflections (red) and occlusions (blue).

color does not signal a change in the geometry. Most of the differences are due to occlusion of different projectors, or cameras (blue). The small, isolated areas on the ball as well as on the body of the angel are due to highly specular reflections in some of the camera-projector patterns (red). At the lower mirroring part of the mug, we have inter-reflection with the ground. Nonetheless, most of the shape up front and on the ground is recovered at high precision. Especially on the ground of the mug, many phase signals are dropped due to inconsistency introduced by the interreflections. This shape would definitively benefit from a more azimuthal camera setting. There are also some inaccuracies in the very dark top area due to high gain used to accelerate the capturing.

For the evaluation of our fine optimization step, we follow the work of Weinmann et al. [24]. The reconstructed point cloud of the cue ball is mapped against a sphere and normalized with respect to the specified diameter of 6.02 cm. We need to stress that we do not perform any removal of outliers, except defining an ROI to crop out the mounting device of the ball. We vary the set of used points dependent on the number of at least visible camera-projector pairs and accepted variance in the result of the fine optimization step. The numbers are reported in Table 1 as RMSE values in µm. These numbers indicate that the number of pairs is an important factor for achieving high accuracy.

Comparing the numbers with Weinmann et al., they achieved an RMSE of 23.3 µm with 51 cameras and 10 projectors. We achieve an RMSE error of down to 13.9 µm for the points visible from almost all cameras and projectors. Even

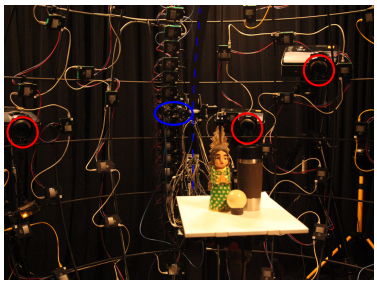

Fig. 5: The test objects in our experimental hardware setup. (Blue: Cameras on the arc. Red: Projectors)

	Cam/Proj-Pairs			
σ^2	8	15	30	45
$\pi/12$	25.2	22.1	18.0	15.0
$\pi/18$	24.9	21.9	17.7	15.0
$\pi/24$	21.9	20.3	17.2	14.9
$\pi/36$	16.1	15.2	14.1	13.9

Table 1: Results of the cue ball evaluation (RMSE values in µm).

when we include less reliable points, the numbers are still comparable, but with much fewer required cameras and projectors. Furthermore, we need to capture only 6 images per projector, whereas their approach would be on 44 for the same projector resolution.

6 Conclusion

We propose an accurate and precise multi-view phase scanning method for robust 3D reconstruction that is able to handle occlusions and optically challenging materials with e.g. subsurface scattering and specular reflections. We demonstrate that optimizing over all cameras, all projectors and all patterns simultaneously improves the overall accuracy significantly. Nonetheless, we only rely on capturing the highest frequency phase shifting patterns. Phase unwrapping with lower frequencies is substituted by a multi-view consistency validation. The final optimization considers the phase of all available SL responses which have been judged to be reliable. The quality of the reconstructed results clearly depends on the number of reliable camera-projector pairs, which strongly indicates that the method fully exploits the available multi-view information for improved accuracy.

While we demonstrate that our combined multi-view and multi-projector approach is able to cope with subsurface scattering and specular reflections, areas of very strong inter-reflections that affect almost all projectors still pose a challenge. The proposed framework is easily extendable with other continuous structured light patterns or even a mixture of different patterns for potentially more reliable detection of correct camera-projector pairs.

Acknowledgement.

This work was supported by the German Research Foundation (DFG): SFB 1233, Robust Vision: Inference Principles and Neural Mechanisms, TP 2.

References

1. Ajdin, B., Finckh, M., Fuchs, C., Hanika, J., Lensch, H.: Compressive higher-order sparse and low-rank acquisition with a hyperspectral light stage. Citeseer (2012)
2. Aliaga, D.G., Xu, Y.: Photogeometric structured light: A self-calibrating and multi-viewpoint framework for accurate 3d modeling. In: Computer Vision and Pattern Recognition, 2008. CVPR 2008. IEEE Conference on. pp. 1–8. IEEE (2008)
3. Aliaga, D.G., Xu, Y.: A self-calibrating method for photogeometric acquisition of 3d objects. IEEE transactions on pattern analysis and machine intelligence 32(4), 747–754 (2010)
4. Blais, F.: Review of 20 years of range sensor development. Journal of Electronic Imaging 13(1) (2004)
5. Chen, T., Lensch, H.P., Fuchs, C., Seidel, H.P.: Polarization and phase-shifting for 3d scanning of translucent objects. In: 2007 IEEE Conference on Computer Vision and Pattern Recognition. pp. 1–8. IEEE (2007)
6. Chen, T., Seidel, H.P., Lensch, H.P.: Modulated phase-shifting for 3d scanning. In: Computer Vision and Pattern Recognition, 2008. CVPR 2008. IEEE Conference on. pp. 1–8. IEEE (2008)
7. Davis, J., Ramamoorthi, R., Rusinkiewicz, S.: Spacetime stereo: A unifying framework for depth from triangulation. In: Computer Vision and Pattern Recognition, 2003. Proceedings. 2003 IEEE Computer Society Conference on. vol. 2, pp. II–359. IEEE (2003)
8. Furukawa, R., Kawasaki, H.: Dense 3d reconstruction with an uncalibrated stereo system using coded structured light. In: Computer Vision and Pattern Recognition-Workshops, 2005. CVPR Workshops. IEEE Computer Society Conference on. pp. 107–107. IEEE (2005)
9. Furukawa, R., Kawasaki, H.: Uncalibrated multiple image stereo system with arbitrarily movable camera and projector for wide range scanning. In: 3-D Digital Imaging and Modeling, 2005. 3DIM 2005. Fifth International Conference on. pp. 302–309. IEEE (2005)
10. Furukawa, R., Sagawa, R., Kawasaki, H., Sakashita, K., Yagi, Y., Asada, N.: One-shot entire shape acquisition method using multiple projectors and cameras. In: Image and Video Technology (PSIVT), 2010 Fourth Pacific-Rim Symposium on. pp. 107–114. IEEE (2010)
11. Garcia, R.R., Zakhor, A.: Consistent stereo-assisted absolute phase unwrapping methods for structured light systems. IEEE Journal of Selected Topics in Signal Processing 6(5), 411–424 (2012)
12. Granados, M., Ajdin, B., Wand, M., Theobalt, C., Seidel, H.P., Lensch, H.P.: Optimal hdr reconstruction with linear digital cameras. In: Computer Vision and Pattern Recognition (CVPR), 2010 IEEE Conference on. pp. 215–222. IEEE (2010)
13. Gühring, J.: Dense 3d surface acquisition by structured light using off-the-shelf components. In: Photonics West 2001-Electronic Imaging. pp. 220–231. International Society for Optics and Photonics (2000)
14. Gupta, M., Agrawal, A., Veeraraghavan, A., Narasimhan, S.G.: Structured light 3d scanning in the presence of global illumination. In: Computer Vision and Pattern Recognition (CVPR), 2011 IEEE Conference on. pp. 713–720. IEEE (2011)
15. Gupta, M., Nayar, S.K.: Micro phase shifting. In: Computer Vision and Pattern Recognition (CVPR), 2012 IEEE Conference on. pp. 813–820. IEEE (2012)
16. Moreno, D., Son, K., Taubin, G.: Embedded phase shifting: Robust phase shifting with embedded signals. In: 2015 IEEE Conference on Computer Vision and Pattern Recognition (CVPR). pp. 2301–2309. IEEE (2015)

17. Nayar, S.K., Krishnan, G., Grossberg, M.D., Raskar, R.: Fast separation of direct and global components of a scene using high frequency illumination. In: ACM Transactions on Graphics (TOG). vol. 25, pp. 935–944. ACM (2006)
18. Nelder, J.A., Mead, R.: A simplex method for function minimization. The computer journal 7(4), 308–313 (1965)
19. Resch, B., Lensch, H.P., Wang, O., Pollefeys, M., Hornung, A.S.: Scalable structure from motion for densely sampled videos. In: CVPR (2015)
20. Salvi, J., Fernandez, S., Pribanic, T., Llado, X.: A state of the art in structured light patterns for surface profilometry. Pattern recognition 43(8), 2666–2680 (2010)
21. Schwartz, C., Sarlette, R., Weinmann, M., Klein, R.: Dome ii: A parallelized btf acquisition system. In: Rushmeier, H., Klein, R. (eds.) Eurographics Workshop on Material Appearance Modeling: Issues and Acquisition. pp. 25–31. Eurographics Association (Jun 2013), http://diglib.eg.org/EG/DL/WS/MAM/MAM2013/025-031.pdf
22. Seitz, S.M., Curless, B., Diebel, J., Scharstein, D., Szeliski, R.: A comparison and evaluation of multi-view stereo reconstruction algorithms. In: 2006 IEEE Computer Society Conference on Computer Vision and Pattern Recognition (CVPR'06). vol. 1, pp. 519–528. IEEE (2006)
23. Srinivasan, V., Liu, H.C., Halioua, M.: Automated phase-measuring profilometry: a phase mapping approach. Appl. Opt. 24(2), 185–188 (Jan 1985), http://ao.osa.org/abstract.cfm?URI=ao-24-2-185
24. Weinmann, M., Schwartz, C., Ruiters, R., Klein, R.: A multi-camera, multi-projector super-resolution framework for structured light. In: 3D imaging, modeling, processing, visualization and transmission (3DIMPVT), 2011 international conference on. pp. 397–404. IEEE (2011)
25. Young, M., Beeson, E., Davis, J., Rusinkiewicz, S., Ramamoorthi, R.: Viewpoint-coded structured light. In: Computer Vision and Pattern Recognition, 2007. CVPR'07. IEEE Conference on. pp. 1–8. IEEE (2007)